

2025-09-25

The self-archived post print version of this conference paper is available at Linköping University Institutional Repository (DiVA):

<https://urn.kb.se/resolve?urn=urn:nbn:se:liu:diva-218067>

Localization Using DVB-T Signals: Experimental Insights and Validation

Joakim Rydell, Anja Hellander, Jacob Eek and Gustaf Hendeby

In: Proceedings of the 2025 28th International Conference on Information Fusion, FUSION 2025, pp. 1-8.

ISBN: 9781037056239

Publisher: IEEE

<https://doi.org/10.23919/FUSION65864.2025.11124006>

N.B.: When citing this work, cite the original publication.

© 2025 IEEE. Personal use of this material is permitted. Permission from IEEE must be obtained for all other uses, in any current or future media, including reprinting/republishing this material for advertising or promotional purposes, creating new collective works, for resale or redistribution to servers or lists, or reuse of any copyrighted component of this work in other works.

Localization using DVB-T Signals: Experimental Insights and Validation

Joakim Rydell^{†*}, Anja Hellander^{‡§*}, Jacob Eek[†] and Gustaf Hendeby[§]

[†] Swedish Defence Research Agency, Linköping, Sweden

e-mail: `firstname.lastname@foi.se`

[‡] Saab Dynamics, Linköping, Sweden

e-mail: `firstname.lastname@saabgroup.com`

[§] Dept. of Electrical Engineering, Linköping University, Linköping, Sweden

e-mail: `firstname.lastname@liu.se`

Abstract—Accurate positioning, navigation and timing (PNT) is important for military and civilian applications alike. In recent years navigation using signals of opportunity (SOPs) has received increased interest as a complement or alternative to Global Navigation Satellite Systems (GNSS).

We previously proposed a localization framework using opportunistic digital television signals. In it, a navigator localizes itself aided by a stationary base station at a known location, using two time difference of arrival (TDOA) measurements and one two-way ranging (TWR) measurement. In this work we implement and evaluate the proposed framework using real measurements, and based on this propose an extended model which includes the difference in clock bias between the navigator and the base station. The experimental results show that the framework can achieve a root mean square error (RMSE) in absolute position of less than 50 m provided that at least three TDOA measurements are used (with or without TWR), and sometimes if only two TDOA measurements are used in combination with a TWR measurement.

We also show experimentally that the transmitter clocks are stable enough for the navigator to extract the TDOA measurements relying only on its own current measurements and previously collected data by the base station. Thus, by replacing the TWR measurement with a third TDOA measurement, the base station need not be active or communicate with the navigator during the localization. In scenarios where communication is undesirable or impossible, this can be advantageous.

Index Terms—Localization, Signals of opportunity, TDOA

I. INTRODUCTION

Accurate positioning, navigation and timing (PNT) is critical for many applications such as emergency services, transportation, surveillance and military defense. To obtain this, Global Navigation Satellite Systems (GNSS) such as GPS, GLONASS, Galileo and Beidou have been the dominating method during the last decades. However, as jamming and spoofing attacks, to which GNSS is vulnerable, have become increasingly common the need for and interest in alternative positioning methods has greatly increased. Such alternative methods include terrain-aided navigation, image-based navigation and navigation using signals of opportunity (SOPs).

This work was partially supported by the Wallenberg Artificial Intelligence, Autonomous Systems and Software Program (WASP), funded by Knut and Alice Wallenberg Foundation, and by the Swedish strategic research center Security Link.

The authors marked with * have contributed equally to this manuscript.

SOPs are signals whose primary purpose is not to aid navigation, but may be opportunistically received and used to navigate [28]. Examples include signals originating from AM/FM radio [9, 22], digital television [29, 38], cellular signals [13, 17, 21] and satellites in low-Earth orbit (LEO) [18, 30] such as Starlink [24, 25], Iridium [20, 31], Orbcomm [36] and Globalstar [41]. These signals are typically more difficult to jam or spoof than GNSS signals, but typically lack (precise) position and timing information as they are not intended for PNT purposes. Navigation frameworks relying on SOPs may therefore need to simultaneously estimate the position and clock error of the navigator as well as the SOP emitters [19].

Of the possible signal sources for SOP, digital television has perhaps been relatively overlooked compared to LEO satellites and cellular signals. Digital television signals lack timing information and are not necessarily synchronized precisely enough between transmitters. However, an advantage is that the locations of digital television transmitters are often known with good precision, unlike, *e.g.*, the positions of LEO satellites which must be estimated.

In this work, we consider a localization problem where a mobile navigator aided by a stationary base station positions itself using time difference of arrival (TDOA) measurements obtained by comparing the arrival times of opportunistic digital television signals as well as two-way ranging (TWR) measurements between the navigator and the base station.

A. Related Work

Using terrestrial digital television signals for localization has been considered before. There are several different international digital television standards that use different transmission technologies [8]. Of these, the European DVB-T [33] is the most widespread with 147 countries currently using DVB-T and/or its next generation DVB-T2 [6]. Other standards include the American ATSC, the Japanese ISDB-T and the Chinese DTMB standards.

A common approach for localization using digital television signals is to extract time of arrival (TOA) measurements to a number of transmitters. This is the approach used in [2–4] that

use DVB-T signals, [11, 14, 35] that use DTMB signals, and [26, 34, 37–39] that use ATSC signals.

Another approach that can be used in single frequency networks, where transmitters are synchronized and transmit the same signals, is to use TDOA measurements computed by comparing the arrival times of the signals from each transmitter [5, 16, 29, 40]. A challenge here is that transmitters in real life are not perfectly synchronized and will have a constant delay which must be estimated [16]. If transmitters send at different frequencies, alternative TDOA measurements can be extracted by introducing a stationary receiver at a known location and measuring the difference in arrival time between the stationary and mobile receivers [1, 10, 29]. A downside with this is that it requires the two receivers to be synchronized and communicate with each other.

A closely related problem is that of positioning using opportunistic cellular mobile phone signals. In [17], a mobile receiver positions itself using pseudorange measurements to cell towers, aided by another receiver which maps transmitter positions and clock error parameters. In [21], the transmitter positions are assumed to be known and the mobile receiver estimates the transmitter clock error parameters without a secondary receiver. Similar to the framework used in this work, a combination of TDOA and TWR measurements are used in [7, 27, 32]. In [27] only a single TWR measurement and a single TDOA measurement are used which is not enough to uniquely determine the position. In [7] TDOA, TWR and direction of arrival (DOA) measurements are combined. In [32] TDOA measurements to stationary transmitters at known and unknown locations are combined with TWR measurements between mobile agents.

B. Contributions

We extend our previous work [10] by implementing the proposed localization framework on hardware and experimentally evaluating its performance on real-life signals collected in Linköping, Sweden. Based on preliminary findings we improve the model used in [10] by extending the state to estimate to include also the difference in clock bias between the mobile and stationary receivers.

Further, we propose an alternative approach where the TWR measurement in [10] is replaced with a third TDOA measurement between the base station and the mobile navigator. We demonstrate in experiments that since the transmitter clocks are stable enough the TDOA measurements can be computed using the data collected by the navigator and previously collected data by the base station. Hence, this approach does not require communication between the base station and the navigator, or even that the base station is active during the same time as the navigator.

II. PROBLEM FORMULATION AND PRINCIPAL SOLUTION

We consider a mobile navigator attempting to estimate its 2D position $\mathbf{p} = (x, y)^T$, aided by a stationary base station located at the known location $\mathbf{p}_B = (x_B, y_B)^T$. The navigator and the base station both receive opportunistic

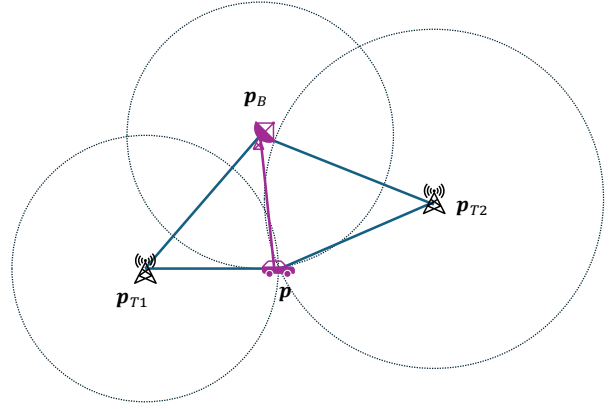


Fig. 1: An overview of the investigated setup. The mobile navigator at \mathbf{p} and the base station at \mathbf{p}_B receive SOPs from two stationary transmitters.

signals from $N \geq 2$ DVB-T transmitters at known locations $\mathbf{p}_{T,n} = (x_{T,n}, y_{T,n})^T$, $n = 1, \dots, N$. This setup is illustrated in Fig. 1. The transmitters do not necessarily transmit signals with the same frequency, and transmitters that transmit with the same frequency are not necessarily synchronized.

For each transmitter $n = 1, \dots, N$ a TDOA ranging measurement z_n can be modelled as

$$z_n = \|\mathbf{p} - \mathbf{p}_{T,n}\| - \|\mathbf{p}_B - \mathbf{p}_{T,n}\| + c\epsilon + e_n, \quad (1)$$

where c is the propagation speed of the signal, ϵ is the difference in clock bias between the navigator and the base station, and $e_n \sim \mathcal{N}(0, \sigma_n^2)$ is an error term.

A TWR measurement between the mobile navigator and the base station is modelled as

$$z_0 = \|\mathbf{p} - \mathbf{p}_B\| + e_0, \quad (2)$$

where $e_0 \sim \mathcal{N}(0, \sigma_0^2)$.

Denote $\mathbf{x} = (x, y, \epsilon)^T = (\mathbf{p}^T, \epsilon)$. In the case where $N = 2$, the measurements can then be modelled as

$$\mathbf{y} = (z_0, z_1, z_2)^T = h(\mathbf{x}) + \mathbf{e}, \quad (3)$$

where

$$h(\mathbf{x}) = \begin{pmatrix} \|\mathbf{p} - \mathbf{p}_B\| \\ \|\mathbf{p} - \mathbf{p}_{T,1}\| - \|\mathbf{p}_B - \mathbf{p}_{T,1}\| + c\epsilon \\ \|\mathbf{p} - \mathbf{p}_{T,2}\| - \|\mathbf{p}_B - \mathbf{p}_{T,2}\| + c\epsilon \end{pmatrix} \quad (4)$$

and

$$\mathbf{e} = (e_0, e_1, e_2)^T \sim \mathcal{N}(\mathbf{0}, \text{diag}(\sigma_0^2, \sigma_1^2, \sigma_2^2)). \quad (5)$$

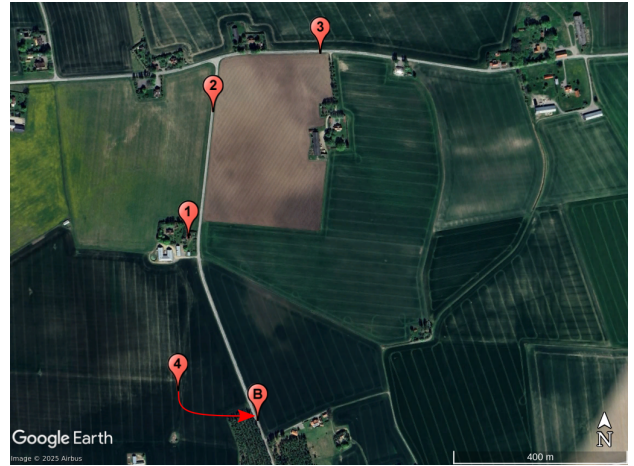
The position and clock bias difference can be estimated using weighted nonlinear least squares (WNLS) as

$$\hat{\mathbf{x}} = \arg \min_{\mathbf{x}} \frac{1}{2} \sum_{k=1}^M (\mathbf{y}_k - h(\mathbf{x}))^T R^{-1} (\mathbf{y}_k - h(\mathbf{x})) \quad (6)$$

where M is the number of measurements and $R = \text{cov}(\mathbf{e}) = \text{diag}(\sigma_0^2, \sigma_1^2, \sigma_2^2)$.



(a) Overview



(b) Zoomed in

Fig. 2: Transmitter and receiver locations. T: DVB-T transmitter, B: stationary TWR base station, Q: stationary DVB-T receiver. (Note, the position 4 is almost collocated with the TWR base station B.)

III. EXPERIMENTS, HARDWARE, AND RADIO MEASUREMENTS

This section presents the experiments performed. It is split into three subsections, detailing aspects related to transmitter and receiver locations, radio-specific aspects, and algorithms for detection and timestamping of signals from each DVB-T transmitter.

A. Experiment Location and Utilized Transmitters

DVB-T and TWR data was collected at five locations (B, 1, 2, 3, and 4), for which DVB-T signals from three transmitters at positions $\mathbf{p}_{T,n}$, $n = 1, 2, 3$, are visible. Additionally, DVB-T data was collected at position Q. B and Q are considered known positions, and are used as reference positions, or base stations, for the DVB-T measurements. Fig. 2 shows these locations; panel (a) provides an overview, while panel (b) focuses on B and 1–4. Note that location 4 is very close to B. The ground truth positions of these locations were measured using GNSS.

When using both DVB-T and TWR for estimation, with Q as reference position for DVB-T, location B is still used as reference position for the TWR measurements. The reason for using different base station locations for DVB-T and TWR is that the system used for TWR (described below) is limited in range. DVB-T, on the other hand, has long range, and performing the experiments at a larger distance from the DVB-T base station is more relevant, as it more closely resembles an typical use case for the presented positioning algorithm.

B. Radio hardware, software and signals

The experiments were performed using three Ettus USRP B200mini¹ software defined radio (SDR) devices, each controlled by GNU Radio² running on Linux computers. One of

these was used as DVB-T base station location (at Q), one as TWR base station (at B), and the last (mobile) one was used at locations 1–4.

DVB-T signals were acquired by the device at Q and the mobile device, by tuning them to the frequencies of the three transmitters and logging raw IQ samples to files, which were later analyzed offline in order to extract timing differences. Two of the transmitters operate at the same frequency, and transmit the same signal. This implies that these transmitters need to be well synchronized in order to avoid interfering with each other; experimental data indicate that the synchronization is stable to within one sample (approximately 0.1 microseconds, or 30 meters) over a period of several weeks. The third transmitter operates at another frequency, and therefore does not need the same level of synchronization. It is, however, also experimentally verified to be accurately synchronized with the other transmitters. This synchronization stability removes the requirement of operating the DVB-T base station and the mobile device simultaneously, since the time differences observed at the base station are essentially constant over time.

TWR measurements were performed using a slightly modified version of gr-lora-sdr [15], which is a FOSS implementation of the LoRa protocol for use with GNU Radio. The procedure follows the basics of LoRa ranging as presented in [23]. Two gr-lora-sdr instances were used: one stationary at location B and one mobile at location 1–4, configured such that the device at B sent periodical PING requests, to which the other one replied. The modifications enabled timestamping of detected LoRa messages. By using both these instances in full duplex mode, they receive both their own transmissions and those sent from the other end, and the range between the two USRPs is given by

$$r = c \cdot \frac{t_B - t_m}{2}, \quad (7)$$

where t_B denotes the time elapsed between ranging request

¹Ettus USRP B200mini: <https://www.ettus.com/all-products/usrp-b200mini/>

²GNU Radio: <http://www.gnuradio.org>

from the stationary base station B, and its response from the mobile station, and t_m denotes processing delay at the mobile station producing a ranging response after having received a request. Since the radios used are not capable of high power output, the range of these measurements is limited to approximately 1 km in line of sight conditions and at the frequency used (869 MHz).

C. DVB-T Signal Detection and Timestamping

The signal properties of DVB-T are described in Appendix A. Signal detection and timestamping was conducted offline and generally follows the method presented in [12]. Symbol detection and extraction from logged RF data was conducted by utilizing that the cyclic prefix (CP) is a replica of the ending of the OFDM symbol, hence by finding the maximum of correlations between groups of N_{cp} samples, the starting sample of the OFDM symbol is collected, and the symbol may be extracted. After symbol extraction, the continual and scattered pilot carriers are extracted. The data transmitted in both types of pilots is given by a known pseudo-random binary sequence (PRBS).

By varying the time offset and searching for correlation maxima between the extracted pilot carriers, and the known PRBS sequence, the time of reception of a signal can be found with subsample accuracy. This also enables detection of multiple correlation peaks, corresponding to signals from multiple transmitters reaching a receiver at slightly different times.

Fig. 3 shows correlation as a function of time offset for the two transmitters operating at the same frequency. Panel (a) shows the correlation peaks observed at Q, while the peaks at B are shown in panel (b). At Q the peaks are clearly separated, while they are very close together at B. Knowing the distance between Q and the transmitter locations, the time offset between the two transmitters can be computed. It turns out that the signals are not transmitted simultaneously, but with a small offset that causes them to reach B (which is not located equally far from the two transmitters) at almost the same time. The figures show one example from each of the two locations. Signals were recorded during approximately one second per frequency at each location, and 250 timestamps per transmitter were extracted from the data.

In the example from Q, the two highest peaks correspond to signals received directly from the two different transmitters. The other peaks are likely caused by multipath propagation, where the signals have bounced off buildings etc. At B, the signals of interest correspond to the peaks at approximately +3 and -17 samples, respectively, while the correlation peaks around +10 samples are likely echoes of the stronger signal. At each location, the two transmitters at the same frequency are detected by finding the two highest peaks with sufficient separation in time. The minimum acceptable separation has been selected for each location in order to exclude echoes of the strongest signal. This manual tuning can easily be omitted if a prior estimate of the receiver location is available (e.g., when using these measurements in a navigation filter).

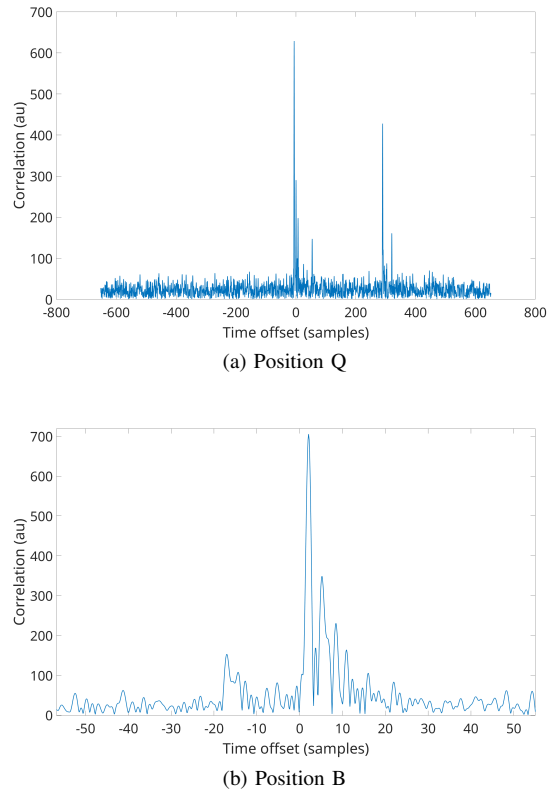


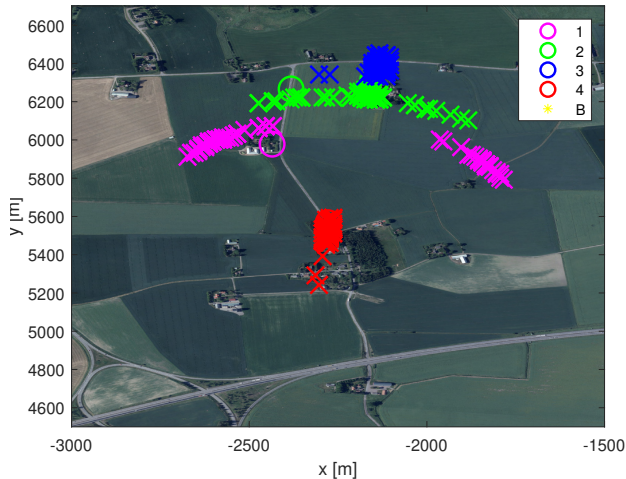
Fig. 3: Correlation between received signal and known pilot carriers, for different time offsets.

Such an estimate also enables association between transmitters and received signals. In these experiments, we assumed prior knowledge about the expected order of the two signals, and used this to associate the signals to their respective transmitters.

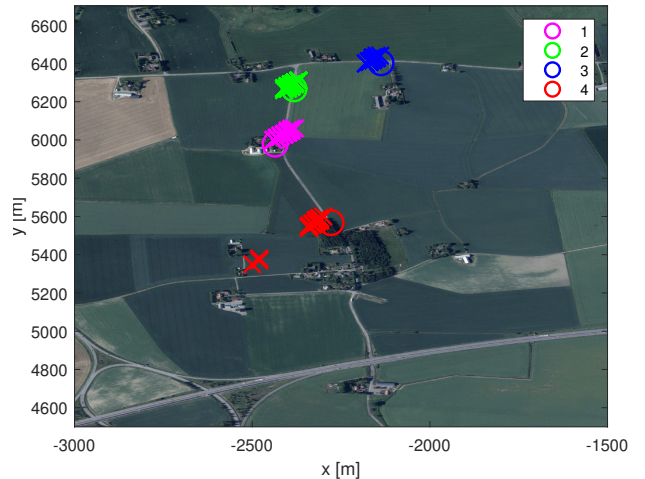
Since the location of scattered pilots is repeated every four symbols, the timestamping of detected signals from each transmitter has an ambiguity corresponding to four times the time per symbol, or approximately 4 ms. From a position estimation point of view, this corresponds to more than 1200 km, and can be easily resolved in most realistic scenarios. The periodic nature of the timestamping also means that all time differences of signal detections from different transmitters, at the reference and mobile receivers, can be computed modulo the period time. Hence, it is not necessary to detect and timestamp the *same* part of a signal in the two receivers. Instead, any detection of the repetitive pilot pattern can be used for positioning.

IV. EXPERIMENTAL RESULTS

For each base station position (B, Q) we estimate the position of 1, 2, 3 and 4 using the collected data. We generate 100 TDOA measurements by randomly selecting which samples to use from the data collected by the base station and the mobile navigator. For the TWR measurements, we use the median of the measurements collected at each



(a) Two TDOA measurements, base station at B



(b) Three TDOA measurements and no TWR, base station at Q

Fig. 4: Ground truth (circles) and resulting estimates (crosses).

position. We consider three combinations of measurements: using the TWR measurement and TDOA measurements for two transmitters (Linköping and Norrköping) as in [10], using the TWR measurement and TDOA measurements for all three transmitters, and using only the TDOA measurements with no TWR measurement. The estimated positions are computed by solving the WNLS problem (6) using grid search, first over a grid with spatial resolution 200 m and then over a finer grid with spatial resolution 10 m centered around the state obtained by the first grid search. Based on the experimental data we select $\sigma_0 = 100, \sigma_1 = \sigma_2 = \sigma_3 = 50$.

A. Results

The RMSE of the resulting estimates when the base station is placed at B is shown in TABLE I. As there are a couple of outliers (2 out of 100 estimates) with errors of several kilometers that skew the results we show also the resulting RMSE with these outliers removed. It can be seen that for positions 1 and 2 using only two TDOA measurements results in an RMSE of several hundred meters even after the removal of outliers. However, using all three TDOA measurements results in an RMSE of less than 50 m with and without the TWR measurement. For positions 3 and 4 it is instead the setup with only two TDOA measurements that performs the best, 44 m and 70 m, respectively. For these positions the difference between the best and worst measurement combination is less pronounced, as using three TDOA measurements results in an RMSE of about 50 m for 3, and around 70 and 120 m for 4.

The RMSE of the resulting estimates when the base station is placed at Q is shown in TABLE II. As previously described, as the distance to Q is too large for the TWR sensor the results reported with Q as base station and TWR measurements still use the TWR measurements to B. It can be seen that for positions 1 and 2 using only two TDOA measurements results in an RMSE of several hundred meters, but for positions 3

TABLE I: Resulting RMSE with base station at position B after outlier removal (2 out of 100 estimates removed). Results in parentheses show the RMSE without outlier removal.

Position	RMSE [m]		
	TWR + 2 TDOA	TWR + 3 TDOA	3 TDOA
1	418.78 (669.55)	49.07 (580.05)	49.21 (694.73)
2	233.75 (566.07)	43.71 (568.48)	49.00 (684.53)
3	44.26 (507.26)	50.56 (558.03)	50.96 (672.90)
4	69.54 (517.42)	88.11 (571.26)	122.09 (698.67)

TABLE II: Resulting RMSE with base station at Q.

Position	RMSE [m]		
	TWR + 2 TDOA	TWR + 3 TDOA	3 TDOA
1	397.15	62.83	49.55
2	227.89	26.36	44.46
3	24.45	30.57	50.73
4	45.00	68.43	89.37

and 4 this is the setup that results in the lowest RMSE, with an RMSE of about 25 m for 3 and 45 m for 4.

The resulting estimates and the ground truth locations for two of the cases are shown in Fig. 4. In Fig. 4a it can be seen that when the base station is placed at B and two TDOA measurements are used, the estimates for 1 and 2 are spread out on a circle arc whereas the estimates for 3 and 4 are closer together and closer to the ground truth. In Fig. 4b three TDOA measurements are used (but no TWR measurement) and the base station is placed at Q. In this case, all positions have estimates close to the ground truth and close together.

B. Discussion

The results presented in this paper demonstrate that the method proposed in [10] can be implemented and that it is possible to achieve an RMSE of around 50 m. However, for two of the positions that were investigated it was necessary to use an additional TDOA measurement to achieve this. The

TWR measurement error is significantly larger (RMSE of around 100 m) compared to the error assumed in [10] (standard deviation < 20 m), so it is likely that an improved accuracy in the TWR sensor would improve the performance further.

When the base station was placed at B there were a few outliers where the estimate was off by several kilometers. As the outliers were relatively few (2 of 100 estimates) they should not be difficult to reject by, *e.g.*, comparing several estimates and rejecting estimates that are too far from the others.

An important observation is that the signal data collected by the base station and the mobile navigator have not been collected at the same time. The results therefore indicate that the transmitter clocks are stable enough that the mobile navigator and the base station do not need to communicate in order to obtain the TDOA measurements as it is sufficient for the mobile navigator to have access to data previously collected by the base station. In a scenario where communication with the base station is impossible or undesirable this can still allow for TDOA measurements even in multifrequency networks where there are not sufficiently many pairs of transmitters transmitting at the same frequency to allow for standard TDOA measurements. This increases the number of transmitters needed to three instead of two. As no actual base station infrastructure is needed at the time of estimation, it also allows for using multiple base stations in the form of previously collected data at a known location. The navigator could then select which base station(s) to use depending on its current location.

V. CONCLUSION AND FUTURE WORK

This section summarizes the paper and the future work.

A. Conclusion

We have considered a localization problem where a mobile navigator localizes itself aided by a stationary base station at a known location. The available measurements are two-way ranging (TWR) between the navigator and the base station, and time difference of arrival (TDOA) measurements obtained by observing the difference in arrival time of digital television signals from transmitters at known locations at the navigator and the base station as described in [10].

We have implemented and evaluated the proposed framework at different locations in the area of Linköping, Sweden using different combinations of TWR and TDOA measurements. The results show that it is possible to achieve a root mean square error (RMSE) of around 50 m, but that this may require at least three TDOA measurements. We have also shown that provided that the transmitter clocks are stable enough, the TDOA measurements can be extracted without actual communication with the base station and that it suffices to have access to previously collected data by the base station as well as the data collected online by the navigator. Our experimental results show that this is the case. This can be an advantage in scenarios where communication is not possible, but it requires the transmitter clocks to be sufficiently stable.

B. Future Work

Future work includes equipping the mobile navigator with an inertial measurement unit (IMU) and estimating the position using an extended Kalman filter (EKF). To do this the clock bias model should be extended to include the drift, which should be estimated as well.

Additional experiments will be performed to better understand for how long the transmitter clocks are stable in order to better evaluate the potential of using only previously collected data instead of a physical base station. Future work could also include investigating the possibility of using several such base stations and perhaps also the possibility of an approach similar to simultaneous localization and mapping (SLAM) where the navigator saves data as it navigates to be used as TDOA reference and simultaneously estimates its own location and that of the reference locations.

Future work will also investigate the effects of multipath interference on the localization accuracy and methods to mitigate this.

APPENDIX

A. DVB-T signal description

DVB-T signals are transmitted using orthogonal frequency-division multiplexing (OFDM), which means that the bandwidth used for transmission is divided into a large number of narrowband subchannels. Data is split into multiple streams, which are sent over these individual channels. OFDM has several advantages, including good tolerance to multipath propagation, where time-shifted echoes of a signal reach a receiver. This situation is highly similar to the case where multiple copies of a signal are sent from different transmitters, and reach a receiver slightly out of synchronization with each other.

Transmitted DVB-T signals are organized into frames, each consisting of $n_s = 68$ OFDM symbols. All DVB-T signals utilized in this paper are in 8K mode, *i.e.*, each OFDM symbol comprises $K = 6817$ subcarriers. In one symbol, each subcarrier represents a complex number, which encodes a few bits of data. The transmitted signal s for one symbol is the FFT of the complex subcarriers, after padding with zeros to fill up 8192 samples. Additionally, the last 1024 samples of s are also inserted at the beginning of the signal, which then becomes $1024 + 8192 = 9216$ samples long. This copy is referred to as a cyclic prefix (CP), and gives rise to the above-mentioned tolerance to multipath propagation. The signal is transmitted at $64/7 \approx 9.14$ Msamples/second, which means that each sample corresponds to approximately $0.1 \mu\text{s}$ or 30 meters of range. Hence, each symbol of 9216 samples has a duration of approximately 1 ms.

The subcarriers contain both user data and pre-defined reference information used to estimate and correct propagation effects on the radio signal, frequency offsets in the receiver, etc. The reference information is placed in *pilot carriers*. For positioning calculation purposes, the pilot carriers are of most interest, since they contain known data. The pilot carriers are

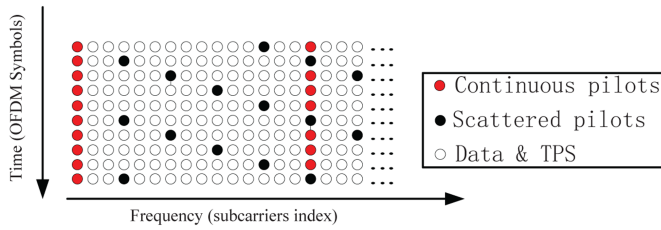


Fig. 5: DVB-T pilot carriers. Figure from [12].

further divided into continual and scattered pilots. Continual pilots are always located on the same subcarriers for all OFDM symbols of the frame, whereas the positions of scattered pilots depend on the location of the symbol in its frame. The locations of the scattered pilots of symbol $i = \{0, 1, \dots, 67\}$ in a DVB-T frame are given by

$$k = 3 \times (i \bmod 4) + 12p, \quad p \in \mathbb{N}, \quad k \in [0, K - 1]. \quad (8)$$

This is illustrated in Fig. 5, and results in the sequence of pilots repeating every 4 symbols.

REFERENCES

- [1] K. L. Carter, R. Ramlall, M. Tummala, and J. McEachen. Bandwidth efficient ATSC TDOA positioning in GPS-denied environments. In *Proceedings of the 2013 International Technical Meeting of The Institute of Navigation*, pages 717–725, 2013.
- [2] L. Chen, O. Julien, P. Thevenon, D. Serant, A. G. Pena, and H. Kuusniemi. TOA estimation for positioning with DVB-T signals in outdoor static tests. *IEEE Trans. Broadcast.*, 61(4):625–638, 2015.
- [3] L. Chen, P. Thevenon, G. Seco-Granados, O. Julien, and H. Kuusniemi. Analysis on the toa tracking with DVB-T signals for positioning. *IEEE Trans. Broadcast.*, 62(4):957–961, 2016.
- [4] L. Chen, L.-L. Yang, J. Yan, and R. Chen. Joint wireless positioning and emitter identification in DVB-T single frequency networks. *IEEE Trans. Broadcast.*, 63(3):577–582, 2017.
- [5] L. Dai, Z. Wang, C. Pan, and S. Chen. Wireless positioning using TDS-OFDM signals in single-frequency networks. *IEEE Trans. Broadcast.*, 58(2):236–246, 2012. doi: 10.1109/TBC.2011.2182431.
- [6] DBV. DTT Deployment Data — DVB — dvb.org. <https://dvb.org/solutions/dtt-deployment-data/>, 2025. [Accessed 21-02-2025].
- [7] Z. Deng, H. Wang, X. Zheng, and L. Yin. Base station selection for hybrid TDOA/RTT/DOA positioning in mixed LOS/NLOS environment. *Sensors*, 20(15):4132, 2020.
- [8] M. El-Hajjar and L. Hanzo. A survey of digital television broadcast transmission techniques. *IEEE Commun. Surveys Tuts.*, 15(4):1924–1949, 2013. doi: 10.1109/SURV.2013.030713.00220.
- [9] S.-H. Fang, J.-C. Chen, H.-R. Huang, and T.-N. Lin. Is FM a RF-based positioning solution in a metropolitan-scale environment? A probabilistic approach with radio measurements analysis. *IEEE Trans. Broadcast.*, 55(3):577–588, 2009.
- [10] A. Hellander and G. Hendeby. On the feasibility of localization using dvb-t signals and combining tdoa and twr measurements. In *2024 27th International Conference on Information Fusion (FUSION)*, pages 1–6, 2024.
- [11] T. Hong, J. Sun, T. Jin, Y. Yi, and J. Qu. Hybrid positioning with DTMB and LTE signals. In *2021 International Wireless Communications and Mobile Computing (IWCMC)*, pages 303–307, 2021.
- [12] J. Huang, L. Lo Presti, and R. Garello. Digital video broadcast-terrestrial (dvb-t) single frequency networks positioning in dynamic scenarios. *Sensors*, 13(8):10191–10218, 2013. doi: 10.3390/s130810191.
- [13] M. Jia, H. Lee, J. Khalife, Z. M. Kassas, and J. Seo. Ground vehicle navigation integrity monitoring for multi-constellation GNSS fused with cellular signals of opportunity. In *2021 IEEE International Intelligent Transportation Systems Conference (ITSC)*, pages 3978–3983, 2021.
- [14] Z. Jiao, L. Chen, X. Lu, Z. Liu, X. Zhou, Y. Zhuang, and G. Guo. Carrier phase ranging with DTMB signals for urban pedestrian localization and GNSS aiding. *Remote Sensing*, 15(2):423, 2023.
- [15] T. Joachim and A. Burg. Design and implementation of lora physical layer in GNU Radio. *Proceedings of the GNU Radio Conference*, 9(1), 2024. URL <https://pubs.gnuradio.org/index.php/grcon/article/view/145>.
- [16] R. Karasek and F. Vejrazka. The DVB-T-based positioning system and single frequency network offset estimation. *Radioengineering*, 27(4):1155–1165, 2018.
- [17] Z. M. Kassas, J. Khalife, K. Shamaei, and J. Morales. I hear, therefore I know where I am: Compensating for GNSS limitations with cellular signals. *IEEE Trans. Signal Process.*, 34(5):111–124, 2017.
- [18] Z. M. Kassas, S. Kozhaya, H. Kanj, J. Saroufim, S. W. Hayek, M. Neinavaie, N. Khairallah, and J. Khalife. Navigation with multi-constellation LEO satellite signals of opportunity: Starlink, OneWeb, Orbcomm, and Iridium. In *2023 IEEE/ION Position, Location and Navigation Symposium (PLANS)*, pages 338–343, 2023.
- [19] Z. M. Kassas, N. Khairallah, and S. Kozhaya. Ad astra: Simultaneous tracking and navigation with megaconstellation LEO satellites. *IEEE Trans. Aerosp. Electron. Syst.*, 2024.
- [20] H. Liang, H. Qin, and H. Li. Doppler compensated pseudorange based signal-of-opportunity positioning using Iridium satellite. *IEEE Transactions on Aerospace and Electronic Systems*, 2024.
- [21] M. Maaref and Z. M. Kassas. Autonomous integrity monitoring for vehicular navigation with cellular signals of opportunity and an IMU. *IEEE Trans. Intell. Transp. Syst.*, 23(6):5586–5601, 2021.
- [22] J. A. McEllroy. *Navigation using signals of opportunity in the AM transmission band*. Master’s thesis, Air Force Institute of Technology, 2006.
- [23] P. Müller, H. Stoll, L. Sarperi, and C. Schüpbach. Outdoor ranging and positioning based on LoRa modulation. In *2021 International Conference on Localization and GNSS (ICL-GNSS)*, pages 1–6, 2021. doi: 10.1109/ICL-GNSS51451.2021.9452277.
- [24] M. Neinavaie and Z. M. Kassas. Unveiling Starlink LEO satellite OFDM-like signal structure enabling precise positioning. *IEEE Transactions on Aerospace and Electronic Systems*, 2023.
- [25] M. Neinavaie, J. Khalife, and Z. M. Kassas. Exploiting Starlink signals for navigation: first results. In *Proceedings of the 34th International Technical Meeting of the Satellite Division of The Institute of Navigation (ION GNSS+ 2021)*, pages 2766–2773, 2021.
- [26] M. Rabinowitz and J. J. Spilker. A new positioning system using television synchronization signals. *IEEE Trans. Broadcast.*, 51(1):51–61, 2005.
- [27] K. Radnosrati, C. Fritsche, F. Gunnarsson, F. Gustafsson, and G. Hendeby. Localization in 3GPP LTE based on one RTT and one TDOA observation. *IEEE Trans. Veh. Technol.*, 69(3):3399–3411, 2020.
- [28] J. F. Raquet, M. M. Miller, and T. Q. Nguyen. Issues and approaches for navigation using signals of opportunity. In *Proceedings of the 2007 National Technical Meeting of The Institute of Navigation*, pages 1073–1080, 2007.
- [29] D. Serant, O. Julien, L. Ries, P. Thevenon, M. Dervin, and G. Hein. The digital TV case-positioning using signals-of-opportunity based on OFDM modulation. *Inside GNSS*, 6(6):pp–54, 2011.
- [30] W. Stock, R. T. Schwarz, C. A. Hofmann, and A. Knopp. Survey on opportunistic PNT with signals from LEO communication satellites. *IEEE Communications Surveys & Tutorials*, 2024.
- [31] Z. Tan, H. Qin, L. Cong, and C. Zhao. New method for positioning using IRIDIUM satellite signals of opportunity. *IEEE Access*, 7:83412–83423, 2019.
- [32] P.-H. Tseng and K.-T. Lee. A femto-aided location tracking algorithm in LTE-A heterogeneous networks. *IEEE Trans. Veh. Technol.*, 66(1):748–762, 2016.
- [33] TSI. Channel coding and modulation for digital terrestrial television. *ETSI EN*, 300(744):V1, 1996.
- [34] X. Wang, Y. Wu, and J.-Y. Chouinard. A new position location system using DTV transmitter identification watermark signals. *EURASIP Journal on Advances in Signal Processing*, 2006(1):042737, 2006.
- [35] X. Wu, C. Zhang, and S. Sohn. Ranging and positioning algorithm based on DTMB system. In *2018 IEEE International Symposium on Broadband Multimedia Systems and Broadcasting (BMSB)*, pages 1–5, 2018.
- [36] Y. Xie, G. Li, H. Qin, C. Zhao, M. Chen, and W. Zhou. Carrier phase tracking and positioning algorithm with additional system parameters based on Orbcomm signals. *GPS Solutions*, 28(4):184, 2024.
- [37] C. Yang and A. Soloviev. Mobile positioning with signals of opportunity in urban and urban canyon environments. In *2020 IEEE/ION Position, Location and Navigation Symposium (PLANS)*, pages 1043–1059, 2020.

- [38] C. Yang, T. Nguyen, D. Qiu, M. Quigley, J. Casper, and B. Wilson. Mobile positioning with DTV signals (ATSC 8VSB and M/H) standards. In *Proceedings of the 25th International Technical Meeting of the Satellite Division of The Institute of Navigation (ION GNSS 2012)*, pages 1208–1216, 2012.
- [39] C. Yang, T. Nguyen, and E. Blasch. Mobile positioning via fusion of mixed signals of opportunity. *IEEE Aerosp. Electron. Syst. Mag.*, 29(4): 34–46, 2014.
- [40] J. Yang, X. Wang, M. J. Rahman, S. I. Park, H. M. Kim, and Y. Wu. A new positioning system using DVB-T2 transmitter signature waveforms in single frequency networks. *IEEE Trans. Broadcast.*, 58(3):347–359, 2012.
- [41] Y. Zhang, H. Qin, and G. Shi. Doppler Positioning Based on Globalstar Signals of Opportunity. In *2023 5th International Conference on Electronic Engineering and Informatics (EEI)*, pages 666–669. IEEE, 2023.